

1 **Responses of neurons in macaque MT to unikinetic plaids**

2

3 Pascal Wallisch and J. Anthony Movshon

4

5 *Center for Neural Science, New York University, 4 Washington Place, New York, NY 10003,*
6 *USA*

7

8 Corresponding author:

9 J. Anthony Movshon
10 Center for Neural Science
11 New York University
12 4 Washington Place
13 New York, NY 10003
14 movshon@nyu.edu

15

16 Abbreviated title: Responses of neurons in macaque MT to unikinetic plaids

17

18

19 Keywords: Motion perception, Motion integration, MT, Electrophysiology, Direction selectivity

20

21 **Acknowledgements**

22 We thank Frédéric Chavane for his comments on an earlier version of the manuscript, Romesh
23 Kumbhani for his help with recordings, and the members of the Movshon lab for their assistance.

24 This work was supported by research grants from NIH to JAM (R01 EY02017, R01 EY04440)
25 and a fellowship from NIH to PW (F32 EY019833). Correspondence and requests for materials
26 should be addressed to J.A.M. (e-mail: movshon@nyu.edu).

27

28 **Abstract**

29

30 Response properties of MT neurons are often studied with “bikinetic” plaid stimuli, which
31 consist of two superimposed sine wave gratings moving in different directions. Oculomotor
32 studies using “unikinetic plaids” in which only one of the two superimposed gratings moves
33 suggest that the eyes first move reflexively in the direction of the moving grating and only later
34 converge on the perceived direction of the moving pattern. MT has been implicated as the source
35 of visual signals that drives these responses. We wanted to know whether stationary gratings,
36 which have little effect on MT cells when presented alone, would influence MT responses when
37 paired with a moving grating. We recorded extracellularly from neurons in area MT and
38 measured responses to stationary and moving gratings, and to their sums: bikinetic and unikinetic
39 plaids. As expected, stationary gratings presented alone had a very modest influence on the
40 activity of MT neurons. Responses to moving gratings and bikinetic plaids were similar to those
41 previously reported, and revealed cells selective for the motion of plaid patterns and of their
42 components (pattern and component cells). When these neurons were probed with unikinetic
43 plaids, pattern cells shifted their direction preferences in a way that revealed the influence of the
44 static grating. Component cell preferences shifted little or not at all. These results support the
45 notion that pattern selective neurons in area MT integrate component motions that differ widely
46 in speed, and that they do so in a way that is consistent with an intersection-of-constraints model.

47

48

49 *New & Noteworthy:* Human perceptual and eye movement responses to moving gratings are
50 influenced by adding a second, static grating to create a “unikinetic” plaid. Cells in MT do not
51 respond to static gratings, but those gratings still influence the direction selectivity of some MT
52 cells. The cells influenced by static gratings are those tuned for the motion of global patterns, but
53 not those tuned only for the individual components of moving targets.

54

55

56 Introduction

57 Neurons in area MT respond selectively to the direction of visual motion (Dubner &
58 Zeki, 1971; Allman & Kaas, 1971), and integrate signals from direction-selective V1 neurons to
59 compute the two-dimensional motion of objects (Movshon et al., 1985; Movshon & Newsome,
60 1996; Simoncelli & Heeger, 1998). The specificity of neuronal responses is limited by what is
61 known as the “*aperture problem*” – if only a single oriented contour of a moving object is in the
62 receptive field (RF), the neuron can only signal motion orthogonal to the orientation of the
63 contour. Because V1 neurons are orientation selective, they respond to contours of a particular
64 orientation and therefore only measure the motion of individual oriented elements and not the
65 true motion of an object containing elements with several orientations. Recovering the velocity
66 of an object requires the integration of multiple moving contours, a process which seems to begin
67 at the level of MT neurons (Movshon et al., 1985; Rodman & Albright, 1987; Khawaja et al.
68 2009). Some MT neurons – component-direction-selective cells – respond to the individual
69 contour components in the stimulus. Others – pattern-direction-selective cells – respond to the
70 two-dimensional motion of the visual pattern (Movshon et al., 1985). Several models have been
71 proposed to account for this behavior of pattern selective neurons in response to two-dimensional
72 motion signals. One early model proposes that MT neurons compute the “intersection of
73 constraints” (IOC) established by local motion measurements (Adelson & Movshon, 1982;
74 Movshon et al., 1985). Each component of the moving pattern imposes a constraint on the
75 coherent motion of a pattern which can be represented by a line in velocity space. The
76 intersection of these constraint lines gives the motion of a coherent pattern and predicts the
77 direction tuning of pattern cells to plaid stimuli (Fig. 1A). The IOC framework is not a model of
78 the neural computation underlying pattern direction selectivity, but a neuronal model has been
79 formulated by Simoncelli and Heeger (1998), and fit to data in a modified form by Rust et al.
80 (2006) and by Nishimoto and Gallant (2011).

81 FIGURE 1 ABOUT HERE

82 Much work on the motion integration properties of MT neurons uses *bikinetic plaids*
83 made by adding two sinusoidal gratings with different orientations, each moving at the same
84 speed (e.g. Movshon et al., 1985; Pack & Born, 2001; Smith et al., 2005; Khawaja et al., 2009).
85 In these stimuli, the direction of the plaid always bisects the direction of the two components,
86 and so corresponds to the direction of their vector mean. By varying the relative speed of the two

87 components, however, one can create plaids whose direction of motion deviates from this mean
88 vector, and in the particular case where one component is stationary, the predicted motion of the
89 resulting *unikinetic* plaid is parallel to the orientation of the stationary grating (Fig. 1B). This
90 case is of interest for models of neuronal integration, because static gratings usually evoke only
91 weak responses from motion sensitive neurons, but both the perceptual experience of motion and
92 the eye movements evoked by it correspond to this prediction (Dobkins, Stoner & Albright,
93 1998; Barthélemy et al. 2008; Quaia et al., 2016), even though the underlying neuronal
94 computation must integrate the motion of two distinct gratings, one moving and one static.

95 We wanted to know whether MT neuronal selectivity would be determined by the true
96 motion of these unikinetic patterns, so we explored this case in single neuron recordings from
97 area MT of macaque monkeys, both awake and under opiate anesthesia. This question was
98 explored by Khawaja et al. (2013), who compared responses to gratings and unikinetic plaids,
99 and found little effect using conventional measures of pattern selectivity. We found that the
100 tuning of component cells in MT was unaffected by the static stimuli, but that of pattern cells
101 was shifted. However, the observed shifts in direction tuning were usually less than expected,
102 and not large enough to make the tuning invariant to the veridical motion of the stimulus. The
103 shifts in direction tuning persisted even if the moving gratings were introduced after the transient
104 responses to static gratings had ended, suggesting a modulatory influence from signals arising
105 outside of MT.

106

107

108 **Materials and Methods**

109

110 *Electrophysiology.* We recorded from well-isolated direction selective neurons in 6 opiate-
111 anesthetized adult male macaque monkeys (*Macaca fascicularis*) (“acute preparation”) and one
112 adult female rhesus monkey (*Macaca mulatta*) that was actively fixating (“awake preparation”).
113 We first describe the methods for the acute preparation, and then describe the differences that
114 pertain to the awake preparation. Our general methods for the surgical preparation of animals,
115 single unit recording and behavioral monitoring in these preparations correspond to those
116 detailed previously (Cavanaugh, 2002; Chukoskie and Movshon, 2009; Jazayeri et al., 2012). All
117 procedures followed the National Institute of Health Guide for the Care and Use of Laboratory
118 Animals, were approved and monitored by the New York University Animal Welfare Committee
119 and complied with the rules and regulations of the USDA.

120

121 *Visual stimuli* were created on an Apple Mac Pro computer and displayed on a gamma-corrected
122 Eizo T966 CRT monitor at a refresh rate of 120 Hz at a mean luminance of 30 cd/m². Stimuli
123 were sinusoidal gratings or plaids of a location, size, spatial and temporal frequency optimized
124 for each cell, presented within a circular aperture surrounded by mean luminance. We presented
125 single sinusoidal gratings – both moving and static – as well as plaids consisting of two
126 superimposed component gratings in 12 directions around the clock. Our plaids were either
127 bikinetic where two moving sinusoidal gratings oriented 120° apart were linearly superimposed
128 (Movshon et al., 1985) or unikinetic plaids that correspond to the bikinetic stimuli in every way
129 except that only one component moved. Stimuli were presented in pseudorandom order in rapid
130 sequence, each for a duration of 330 ms followed by 170 ms of mean luminance. Gratings had a
131 Michelson contrast of 0.5, whereas plaids had a contrast of 1.0. Each stimulus condition was
132 repeated 10-30 times per cell.

133

134 *Recording procedure and behavior.* Prior to recording, we determined that our electrode tip was
135 in MT, both by monitoring the well established landmarks and white/grey matter transitions as
136 the electrode was advanced to MT, as well as observing the classical physiological response
137 characteristics of MT neurons – compact contralateral receptive fields, strong direction
138 selectivity, and the expected range of receptive field sizes for the given eccentricity (Gattass &

139 Gross 1981, Maunsell & van Essen 1983, Albright 1984). In the acute preparation, we placed
140 electrolytic lesions at the conclusion of each experiment, permitting us to verify our recording
141 locations in the superior temporal sulcus. On encountering a neuron, we isolated the spike
142 waveform using a digital window discriminator and mapped the location of the receptive field;
143 most of our receptive field centers were located 3-10 deg from the fovea. We established the
144 preferred eye and presented the stimuli monocularly, covering the non-dominant eye. We then
145 determined the neuron's preferences for the direction of motion, temporal and spatial frequency
146 using full contrast sinusoidal gratings, and proceeded with data recording using uni- and
147 bikinetic plaid stimuli. The distance to the monitor varied between 57 to 114 cm, and the screen
148 therefore subtended between 39° and 20°. To estimate the baseline firing rate of a given neuron,
149 7.5% of the stimulus presentations were blanks consisting of 330 ms of mean luminance.

150
151 *Quantification of neuronal responses to plaids.* We used standard methods (Movshon et al.,
152 1985) to compute the partial correlation of the actual response to plaids with the predictions of
153 idealized models of pattern and component direction selectivity (r_p and r_c , respectively). The
154 predicted pattern model response was simply the measured grating tuning curve, suitably rotated.
155 The predicted component model response was the sum of the two baseline-subtracted grating
156 direction tuning curves, each shifted by an amount appropriate for the plaid angle. To stabilize
157 the variance of these correlations we converted the values to Z-scores (Fisher, 1915; Fisher,
158 1921). For all cells, we computed Z_p and Z_c – the Z-transforms of r_p and r_c – from the responses
159 to gratings and plaids. Cells for which Z_c reliably exceeded both Z_p and 0 were classified as
160 component cells, whereas cells for which Z_p reliably exceeded Z_c and 0 were classified as pattern
161 cells. We computed a *pattern index* as $Z_p - Z_c$.

162
163 For bikinetic plaids, the difference between the peaks of the pattern prediction and each lobe of
164 the component prediction is 60°. For unikinetic plaids, the difference between the pattern and
165 component prediction is only 30° (Fig. 2A). Because most MT cells are broadly tuned for
166 direction, the distinction between the responses of pattern and component cells to unikinetic
167 plaids was often difficult to detect. We addressed this problem in two ways. First, we included
168 two distinct sets of unikinetic plaids, “right-handed” and “left-handed”, in which one or the other
169 grating was static. We then took the mean of two computations of Z_c and Z_p for each cell.

170 Second, we took advantage of these two conditions to examine the rotation of the direction
171 tuning curve that resulted when one plaid component was static. For component cells, the model
172 predicts shifts of tuning 30° clockwise for one condition and 30° anticlockwise for the other. For
173 pattern cells, the model predicts that direction tuning should be invariant to the choice of static
174 grating (Fig. 2A). We measured the tuning curve shifts by rotating the responses to the left-
175 handed and right-handed unikinetic plaids to determine the angle that maximized their
176 correlation, and took this value as the *direction tuning rotation*, a figure of merit for the pattern
177 motion computation for unikinetic stimuli. We also computed this rotation by measuring the
178 angular difference in the summed response vectors (O’Keefe and Movshon, 1998) for the two
179 unikinetic plaid cases; both measures correlated closely ($r=0.87$).

180
181 *Dynamics.* We also included responses to two unikinetic plaids in which the static and moving
182 component gratings were presented with asynchronous onsets. In one condition, the static grating
183 was leading the moving one by 50 ms, in the other one by 100 ms. We analyzed the data from
184 these conditions in sliding 5 ms bins, calculating the vector mean and firing rate for each bin. We
185 calculated the direction tuning rotation for each bin by comparing the vector mean for this bin
186 with the mean tuning for a single moving grating. We then determined the average direction
187 tuning rotation over neurons by calculating the vector mean, weighting the contribution of each
188 neuron by the square root of its firing rate.

189
190 *Recordings from the alert animal.* To accommodate the generally higher temporal frequency
191 preferences in the awake preparation (Alitto et al., 2011), we used an Iiyama HM204DTA CRT
192 monitor with a refresh rate of 200 Hz. The animal viewed the stimuli binocularly from a distance
193 of 57 cm, at which the screen subtended 39° ; we monitored eye movements with an infrared
194 camera system (Eyelink 1000, SR Research). Each trial began with the presentation of a central
195 white spot (diameter 0.2°) for the animal to fixate. Once fixation started, the stimulus sequence
196 commenced, and the animal received periodic liquid rewards.. If the animal moved its gaze more
197 than 1° away from the fixation point, stimulus presentation and reward delivery ceased. Once the
198 animal refixated, stimulus presentation resumed.

199

200 **Results**

201
202 We recorded from 239 neurons. We used direction tuning rotation to detect and exclude 34
203 neurons with unreliable tuning (peak correlations of $r < 0.82$ or a bootstrap-derived standard
204 deviation of more than 25°), from further analysis. Thus, we analyzed the responses of 205 units
205 in area MT, 84 from the 6 anesthetized monkeys, and 121 from the awake monkey.

206 After determining the response preferences of each neuron, we measured its response to five
207 stimulus families. Figure 2A shows schematics of the responses expected from idealized pattern
208 and component cells to these five stimulus families. The first column shows response to static
209 flashed gratings at different orientations. The second and third columns show the “standard”
210 comparison of responses to moving gratings and bikinetic plaids (Movshon et al., 1985; Smith et
211 al., 2005). The fourth and fifth columns show responses to the left- and right-handed unikinetic
212 plaids (see *Methods*). The responses of four representative example neurons to these stimulus
213 conditions are shown in Fig 2B-E. Figure 2B shows data from a component neuron, the shape of
214 whose tuning for bikinetic plaids (black symbols) closely matches the component prediction
215 (blue dashed lines). Figure 2C shows data from a neuron with mixed properties. Figures 2D-E
216 show data from pattern neurons, in which the shapes of the plaid tuning curves more closely
217 match the pattern predictions.

218

219 FIGURE 2 ABOUT HERE

220

221 The component predictions (blue) for bikinetic plaids are computed from sums of the data in the
222 second column, suitably rotated. Component predictions for unikinetic plaids are computed from
223 sums of data in the first column (responses to static gratings, typically weak and poorly tuned),
224 and the second column. The pattern predictions (red) are simply 30° rotations of the tuning
225 curves to moving gratings in the second column. Inspection of the data for the component cell
226 (first row), showed a good correspondence between the tuning for unikinetic plaids and the
227 prediction from the summed responses. In other words, this cell responded to the unikinetic
228 plaids more or less as if the static component were absent. The cell in the second row (“mixed”),
229 which appeared to be pattern selective when tested with bikinetic plaids, shows component-
230 selective-type responses to unikinetic plaids, similar to the cell whose data are shown in the first

231 row. The remaining two pattern cells (bottom two rows), showed responses to unikinetic plaids
232 which were closer to the pattern predictions (red) than to the component predictions.

233

234 FIGURE 3 ABOUT HERE

235

236 Figure 3 shows the distribution of the Z-transformed partial correlations Z_p and Z_c for the neurons
237 in our sample for both bikinetic (Fig. 3A) and unikinetic plaids (Fig. 3B). Figure 3A shows that
238 the distribution of neural response characteristics for bikinetic plaids was similar to those
239 previously reported in MT (Movshon et al., 1985; Smith et al., 2005; Rust et al., 2006; Khawaja
240 et al, 2009): 58 pattern cells (28%, red), 58 component cells (28%, blue), and 89 unclassified cells
241 (43%, black). The four example neurons whose data are shown in Fig. 2 are indicated with black
242 circles. The data from awake recordings are shown with solid symbols while those from
243 anesthetized animals are shown with open symbols. Anesthesia had no effect on the distribution
244 of pattern and component direction selectivity (Movshon et al., 2003).

245

246 Figure 3B shows the distribution of neuronal classifications based on data obtained from the
247 same neurons with unikinetic plaids. Data are colored as they were in Fig. 3A. The data are
248 shifted wholesale down and to the right. By this measure, only a few neurons were “truly”
249 pattern selective, in that they retained their selectivity when unikinetic plaids were used. But this
250 classification method works poorly when the two predictions being distinguished are very
251 similar. Consider Fig. 2, and note the small difference between the predictions for pattern and
252 component cell responses to unikinetic plaids. In the face of normal response variability,
253 differences of this magnitude can be difficult to distinguish, which makes classification
254 challenging.

255

256 It is therefore not surprising that many neurons previously classified as either pattern or
257 component direction selective with bikinetic plaids appear unclassified when tested with unikinetic
258 plaids. This effect was more prominent in pattern cells, probably because their direction tuning
259 tends to be broader than component cells’ (Smith et al., 2005). In quantitative terms, only 7 of
260 the 205 cells (3%) of the total sample were pattern direction selective under conditions of
261 unikinetic stimulation. Component cells under these conditions numbered 107, 52% of the total

262 sample. Finally, the proportion of unclassified cells remained essentially unchanged at 44%. To
263 summarize, there appear to be dramatic shifts away from the pattern category when responses are
264 measured with unikinetic plaids. This observation is consistent with a report by Khawaja et al.
265 (2013), who noted a qualitatively similar shift from pattern to component selectivity in MT
266 neurons, when probing them with unikinetic plaids. But this analysis underestimates the true
267 amount of pattern motion information in the responses of MT cells to unikinetic plaids.

268
269 We realized that the essential feature of pattern selectivity for unikinetic plaids is that the
270 neuronal tuning should remain invariant to the composition of the plaid, whereas component-
271 selective neurons' tuning should shift 30° counter-clockwise for the left-handed plaid and 30°
272 clockwise for the right-handed plaid, 60° in all (Fig. 2A). We decided to use this doubled shift
273 (hereafter “direction tuning rotation”) in preferred direction as a figure of merit by comparing the
274 empirical response of MT neurons to these predictions.

275

276

FIGURE 4 ABOUT HERE

277

278 Figure 4 shows this direction tuning rotation plotted against the pattern index measured with
279 bikietic plaids. An ideal component cell whose tuning curve shifted by the full 30° for each
280 unikinetic plaid would have a direction tuning rotation of 60°, assuming that the response to
281 static gratings was unselective, as was typical (Fig. 2), its directional preference would be
282 determined by the moving component. An ideal pattern cell would show no shift and would have
283 a direction tuning rotation of 0°—its response would be determined by the true motion of the
284 plaid. The data in Fig. 5 show the expected negative slope, and the correlation is highly
285 significant ($r = -0.39$, $n = 205$, $p < 0.0001$). On closer examination, many component cells
286 behave as expected, with direction tuning rotations near 60°. Few pattern cells have direction
287 tuning rotations near 0°; instead, most (like the example cells whose data are presented in Fig. 2)
288 show incomplete shifts in direction preference toward the direction defined by the static grating.
289 It is as if the pattern direction selective ideal for these cells can only be imperfectly approximated
290 when one of the component gratings is static.

291

292 The data from anesthetized and alert recordings (orange and green) were subtly different, with

293 data from alert recordings showing a more pronounced negative slope. This difference is
294 captured by the fitted lines, computed based on the bootstrapped standard deviations of the
295 values (error bars). The difference in the slopes approaches but fails to reach significance in a
296 permutation test ($p = 0.0759$). Full pattern motion coding for unikinetic stimuli – here indicated
297 by direction tuning rotations near 0° – is however evident only for data from alert animals, but
298 the variability of the data could obscure a similar representation under anesthesia.

299

300 In Fig 2, we showed that static gratings presented alone evoked only weak responses from MT
301 cells, yet for pattern direction selective cells they had a potent influence on directional
302 preference. We noticed that the response to static gratings was not only weak but transient,
303 disappearing within 50-100 ms. We therefore decided to examine the time course of the static
304 grating's influence on direction tuning, by delaying the onset of the moving grating and
305 measuring the variation in direction tuning over time; conceptually similar measurements on
306 ocular following behavior were made by Quaia et al. (2016), though they used flickering rather
307 than static stationary gratings.

308

309

FIGURE 5 ABOUT HERE

310

311 Figure 5 shows the design and results of this experiment. In panel A we represent the
312 experimental design: at the start of each trial we switched on a static grating. In one condition,
313 we left that grating on screen for 250 ms. In three other conditions, we added a moving grating –
314 either synchronously, with 50 ms delay, or with 100 ms delay. We took all the data – from 84
315 neurons recorded from anesthetized animals and 121 neurons recorded from the alert animal –
316 and extracted the responses for the condition in which the moving grating moved in the cell's
317 preferred direction. Panels B and C show (for alert and anesthetized data respectively) the mean
318 of the responses of the neuronal population. The mean response to the static grating alone (gray),
319 showed a brief transient that returned to baseline roughly 100 ms after stimulus onset. The
320 responses to the static-moving compound gratings (colors) were all elevated above the response
321 to the static grating alone, and all converged on the same elevated value by the end of the
322 measurement, 250 ms after stimulus onset.

323

324 As described in *Methods*, we rotated the data for each cell so that the preferred direction for
325 gratings was aligned (drawn as rightward in panel A, and denoted as 30° for consistency with Fig
326 4). We then computed the population vector preferred direction, and compared it to that of a
327 moving grating presented alone. The traces of this “tuning rotation” for the three compound
328 stimuli are shown for alert and anesthetized recordings in panels D and E. We averaged data
329 from all cells: pattern, component, and unclassified – separate analysis of these cell groups did not
330 reveal a different pattern of dynamics. The population preferred direction, as indicated by the
331 arrows, therefore falls between the value of 30° corresponding to the pure component direction
332 (horizontal), and 0° corresponding to the pure pattern direction (oblique). The population
333 preferred direction is stably maintained from the onset of tuning to the end of the measurement
334 period. Note that the population preferred direction is the same whether the moving grating is
335 synchronous with the static grating (red trace), or is delayed by either 50 ms (blue) or 100 ms
336 (cyan). It is especially striking to note that for the 100 ms condition, the neuronal response to the
337 static grating had completely ended (panels B and C, gray), yet the influence of this static
338 component on the population preferred direction was undiminished.

339

340 These results raise the question of how the shift in preferred direction produced by the static
341 grating is mediated, since it evokes no response. From this plot, it seems clear that it cannot be
342 mediated by spiking in MT itself, suggesting the involvement of neurons in other areas in the
343 encoding of the direction of unikinetic plaids, perhaps neurons in the ventral stream of visual
344 processing that exhibit a more sustained response to static stimuli.

345

346

347 **Discussion**

348

349 We extended the exploration of pattern motion sensitivity in MT neurons. Unlike their afferents
350 from V1, some MT neurons combine motion signals in a way that makes them sensitive to the
351 motion of compound stimuli. This renders pattern cells, at least in the ideal case, sensitive only
352 to the direction but not to the spatial composition of the moving stimulus. This invariant
353 sensitivity is captured by measuring responses to gratings and to plaids made by summing two
354 gratings; in most previous studies those two gratings have moved at the same speed to create
355 bkinetic or “type I” plaids (Movshon et al., 1985; Rodman and Albright, 1987; Wilson et al.,
356 1992; Rust et al., 2006; Khawaja et al, 2009). Here we have included unikinetic plaids, in which
357 only one of the component gratings moves. These “type II” plaids have the interesting property
358 that their direction of motion deviates from the sum of the motion vectors of their components,
359 and have been used extensively in both perceptual and oculomotor experiments (Ferrera &
360 Wilson, 1987; Ferrera & Wilson, 1990; Wilson et al., 1992; Yo & Wilson 1992; Barthelemy et
361 al., 2008, 2009). They are conceptually similar to “barber pole” stimuli, in which the direction of
362 motion of an oblique grating follows the borders of a narrow bounding window (Guilford, 1929;
363 Wallach, 1935; Adelson & Movshon, 1983; Masson et al., 2000).

364

365 Unikinetic plaids are more than mere parametric extensions of conventional plaids. They are
366 interesting for the exploration of motion integration, because they create cases in which the
367 percept of a moving stimulus is modified by a static one. We wanted to know whether the
368 striking perceptual effects reported with these stimuli were reflected in the responses of neurons
369 in MT: MT neurons compute pattern motion for bkinetic plaids in which both components
370 evoke responses independently; we wondered whether they would also compute pattern motion
371 when one component is static, as MT neurons respond poorly to stimuli that do not move.

372

373 Our results show that the responses of MT pattern cells are indeed influenced by static targets in
374 the receptive field, even though these evoke weak responses by themselves; this influence is not
375 seen for component neurons. However, this effect is not easy to detect with conventional
376 methods for classifying pattern direction selectivity, because the response of MT neurons to
377 static stimuli is weak, which renders predictions based on the response to the static component

378 unreliable. Thus, the standard analysis of the shapes of tuning curves for plaids and their
379 component gratings works poorly when one of the gratings is static (Fig. 3), leading to the false
380 impression that stopping the motion of one grating turns most MT cells into component cells. A
381 more sensitive measure of pattern motion sensitivity in unikinetic plaids is the angle by which
382 the preferred direction is rotated by the addition of a static grating (Fig. 4). Whereas the
383 comparison of tuning in the standard analysis (Fig. 3) depends on shape details for two similar
384 curves, the tuning rotation measure requires only an estimate of preferred direction and is
385 therefore less vulnerable to noise. As considerable variability can always be expected to be
386 present (Taouali et al., 2015), tuning rotation is a more robust and thus more suitable metric of
387 neural responses to bi-kinetic vs. unikinetic plaids. Pattern cells approach but rarely achieve
388 perfect invariance in their direction tuning for unikinetic plaid stimuli, but they approach that
389 ideal for moving stimuli in general. These results are broadly consistent with those of Pack et al
390 (2004), who observed shifts in the tuning of MT responses to “barber-pole” stimuli, but did not
391 distinguish pattern from component cells.

392

393 Our findings have implications for functional theories of the properties of neurons in area MT.
394 Simoncelli and Heeger (1998) proposed that the responses of pattern cells in MT could be
395 accounted for by assuming that they pool the responses of a set of V1 afferents whose selectivity
396 for spatiotemporal frequency is arranged so that they tile the plane in 3-dimensional spatio-
397 temporal frequency space that corresponds to a particular direction and speed of motion. The
398 original characterization of pattern direction selectivity with plaids (Movshon et al., 1985) probes
399 the tiling of this plane by testing two components of the same velocity, leaving much of this
400 stimulus space unexplored. Efforts to characterize the complete three-dimensional frequency
401 structure of the inputs to pattern cells have suggested that the tiling of this plane is often
402 incomplete, being attenuated near the zero-temporal-frequency plane where static stimuli reside
403 (Nishimoto and Gallant, 2011; Zaharia et al., 2019). This may not be unexpected. V1 neurons
404 that provide much of the input to MT are directionally selective and respond poorly to static
405 stimuli (Movshon and Newsome, 1996). Also, pattern neurons in MT respond poorly to stimuli
406 that do not move (Rodman and Albright, 1987; Rust et al. 2006; see Fig. 2 and 5).

407

408 Our results suggest that the responses of pattern cells do reflect information from cells

409 responding to static stimuli (near-zero temporal frequency), but they do so both implicitly and
410 incompletely. The results in Fig 5 show that static gratings evoke a transient response which falls
411 rapidly back to baseline, yet the influence of those static gratings on direction preference persists.
412 This influence must therefore be implicit and nonlinear, and might reflect a modulatory influence
413 from cells which respond better to the static stimuli than MT cells do. It is interesting to
414 speculate about the source of this sustained signal, which might arise from a parallel cortical
415 stream (e.g. through V2, Ponce et al., 2008), or from direct thalamic input to MT from the
416 koniocellular LGN (Sincich and Horton, 2004). Moreover, as shown by Khawaja et al. (2013),
417 pattern responses are more robust in MST than in MT – it is unclear how MST would receive
418 this signal: Directly, from MT or indirectly, from a yet to be characterized path or from both?
419 The influence of the static grating in MT is also incomplete, because only in rare cases do MT
420 cells show completely invariant direction tuning (Fig. 4). Consider the neurons whose pattern
421 index is much greater than zero, the unambiguous pattern cells. If these cells all integrated zero-
422 temporal-frequency information perfectly, they would all have direction tuning rotation values
423 near 0° . In reality, their direction tuning rotations are dispersed over the entire range from 0° to
424 60° – few neurons exhibit the idealized pattern of responses that could be expected from the
425 Simoncelli-Heeger model.

426

427 Finally, we note that our results were qualitatively similar in both acute and awake preparations,
428 despite rather different dynamics and response magnitudes (evident in Fig. 5, cf Alitto et al.,
429 2011). This similarity suggests that attentional or top-down effects, which are diminished or
430 absent in anesthetized animals, had little influence on the general pattern of results.

431

432 How might our results relate to human perception and visually-guided action? Humans misjudge
433 the motion of briefly-presented lines to be orthogonal to their orientation (Lorenceanu et al.,
434 1993). Moreover, measurements of short-latency ocular following in humans and monkeys
435 reveal that the initial tracking of the motion of unikinetic plaids is in the direction orthogonal to
436 the moving component; then, after 10-20 ms, the direction of tracking rotates to match the true
437 pattern motion (Barthelemy et al, 2008, 2009). Our results show, as expected, that component
438 cells can only provide a signal to drive eye tracking of the direction of the moving single grating,
439 while pattern cells could in principle signal the true direction of motion. If the responses of

440 pattern cells were delayed compared to those of component cells, then both the perceptual and
441 the ocular following results could be explained. Interestingly, in earlier work from our laboratory
442 (Smith et al., 2005), we showed that component cells have slightly shorter visual latencies than
443 pattern cells, and further showed that pattern cells' tuning does not fully stabilize for some time
444 after response onset. Our conclusions are therefore consistent with the hypothesis that signals
445 from MT cells contribute to the perception of motion and to the control of visually guided action.
446
447

448 **References**

449

450 Adelson, E. H. & Movshon, J. A. (1982). Phenomenal coherence of moving visual patterns.
451 *Nature*, 300(5892), 523-525.

452 Adelson, E. H. & Movshon, J. A. (1983, April). The perception of coherent motion in two-
453 dimensional patterns. In *proceedings of the Association of Computing Machinery*
454 *Interdisciplinary Workshop on Motion: Representation and Perception, Toronto, Canada.*

455 Albright, T. D. (1984). Direction and orientation selectivity of neurons in visual area MT of the
456 macaque. *Journal of Neurophysiology*, 52(6), 1106-1130.

457 Alitto, H. J., Rathbun, D. L. & Martin Usrey, W. (2011). A comparison of visual responses in the
458 lateral geniculate nucleus of alert and anaesthetized macaque monkeys. *The Journal of*
459 *Physiology*, 589(1), 87-99.

460 Allman, J. M. & Kaas, J. H. (1971). A representation of the visual field in the caudal third of the
461 middle temporal gyrus of the owl monkey (*Aotus trivirgatus*). *Brain Research*, 31(1), 85-105.

462 Barthélemy, F. V., Perrinet, L. U., Castet, E. & Masson, G. S. (2008). Dynamics of distributed
463 1D and 2D motion representations for short-latency ocular following. *Vision Research*, 48(4),
464 501-522.

465 Barthélemy, F. V., Fleuriet, J. & Masson, G. S. (2009). Temporal dynamics of 2D motion
466 integration for ocular following in macaque monkeys. *Journal of Neurophysiology*, 103(3),
467 1275-1282.

468 Cavanaugh, J. R., Bair, W. & Movshon, J. A. (2002). Nature and interaction of signals from the
469 receptive field center and surround in macaque V1 neurons. *Journal of Neurophysiology*,
470 88(5), 2530-2546.

471 Chukoskie, L. & Movshon, J. A. (2009). Modulation of visual signals in macaque MT and MST
472 neurons during pursuit eye movement. *Journal of Neurophysiology*, 102(6), 3225-3233.

473 Dobkins, K. R., Stoner, G. R. & Albright, T. D. (1998). Perceptual, oculomotor, and neural
474 responses to moving color plaids. *Perception*, 27(6), 681-709.

475 Dubner, R. & Zeki, S. M. (1971). Response properties and receptive fields of cells in an
476 anatomically defined region of the superior temporal sulcus in the monkey. *Brain Research*,
477 35(2), 528-532.

478 Ferrera, V. P. & Wilson, H. R. (1987). Direction specific masking and the analysis of motion in

479 two dimensions. *Vision Research*, 27(10), 1783-1796.

480 Ferrera, V. P. & Wilson, H. R. (1990). Perceived direction of moving two-dimensional patterns.
481 *Vision Research*, 30(2), 273-287.

482 Fisher, R. A. (1915). Frequency distribution of the values of the correlation coefficient in
483 samples from an indefinitely large population. *Biometrika*, 10(4), 507-521.

484 Fisher, R. A. (1921). On the probable error of a coefficient of correlation deduced from a small
485 sample. *Metron*, 1, 3-32.

486 Gattass, R. & Gross, C. G. (1981). Visual topography of striate projection zone (MT) in posterior
487 superior temporal sulcus of the macaque. *Journal of Neurophysiology*, 46(3), 621-638.

488 Guilford, J. P. (1929). Illusory Movement from a Rotating Barber Pole. *American Journal of*
489 *Psychology*, 41, 686.

490 Jazayeri, M., Wallisch, P. & Movshon, J. A. (2012). Dynamics of macaque MT cell responses to
491 grating triplets. *Journal of Neuroscience*, 32(24), 8242-8253.

492 Khawaja, F. A., Tsui, J. M. & Pack, C. C. (2009). Pattern motion selectivity of spiking outputs
493 and local field potentials in macaque visual cortex. *Journal of Neuroscience*, 29(43), 13702-
494 13709.

495 Khawaja, F. A., Liu, L. D. & Pack, C. C. (2013). Responses of MST neurons to plaid stimuli.
496 *Journal of Neurophysiology*, 110(1), 63-74.

497 Lorenceau, J., Shiffrar, M., Wells, N. & Castet, E. (1993). Different motion sensitive units are
498 involved in recovering the direction of moving lines. *Vision Research*, 33(9), 1207-1217.

499 Masson, G. S., Rybarczyk, Y., Castet, E. & Mestre, D. R. (2000). Temporal dynamics of motion
500 integration for the initiation of tracking eye movements at ultra-short latencies. *Visual*
501 *Neuroscience*, 17(5), 753-767.

502 Maunsell, J. H. & Van Essen, D. C. (1983). Functional properties of neurons in middle temporal
503 visual area of the macaque monkey. I. Selectivity for stimulus direction, speed, and
504 orientation. *Journal of Neurophysiology*, 49(5), 1127-1147.

505 Movshon, J. A., Adelson, E. H. , Gizzi, M. S. & Newsome, W. T. (1985). The analysis of
506 moving visual patterns. In *Pattern Recognition Mechanisms*, ed. C. Chagas, R. Gattass and C.
507 Gross (*Pontificiae Academiae Scientiarum Scripta Varia* 54: 117–151). Rome: Vatican Press.

508 Movshon, J. A. & Newsome, W. T. (1996). Visual response properties of striate cortical neurons
509 projecting to area MT in macaque monkeys. *Journal of Neuroscience*, 16(23), 7733-7741.

510 Movshon, J. A., Albright, T. D., Stoner, G. R., Majaj, N. J. & Smith, M. A. (2003). Cortical
511 responses to visual motion in alert and anesthetized monkeys. *Nat Neurosci*, 6(1), 3.

512 O'Keefe, L. P. & Movshon, J. A. (1998). Processing of first- and second-order motion signals by
513 neurons in area MT of the macaque monkey. *Visual Neuroscience* 15: 305–317.

514 Nishimoto, S. & Gallant, J. L. (2011). A three-dimensional spatiotemporal receptive field model
515 explains responses of area MT neurons to naturalistic movies. *Journal of Neuroscience*,
516 31(41), 14551-14564.

517 Pack, C. C., Berezovskii, V. K. & Born, R. T. (2001). Dynamic properties of neurons in cortical
518 area MT in alert and anaesthetized macaque monkeys. *Nature* 414: 905-908.

519 Pack, C. C., Gartland, A. J. & Born, R. T. (2004). Integration of contour and terminator signals
520 in visual area MT of alert macaque. *Journal of Neuroscience*, 24(13), 3268-3280.

521 Ponce, C. R., Lomber, S. G., & Born, R. T. (2008). Integrating motion and depth via parallel
522 pathways. *Nature Neuroscience*, 11(2), 216.

523 Press, W. H., Teukolsky, S. A., Vetterling, W. T. & Flannery, B. P. (1992). Numerical recipes
524 2nd edition: The art of scientific computing. Cambridge University Press. Chapter 15.3.

525 Quaia, C., Optican, L. M., & Cumming, B. G. (2016). A motion-from-form mechanism
526 contributes to extracting pattern motion from plaids. *Journal of Neuroscience*, 36(14), 3903-
527 3918.

528 Rodman, H. R. & Albright, T. D. (1987). Coding of visual stimulus velocity in area MT of the
529 macaque. *Vision Research*, 27(12), 2035-2048.

530 Rust, N. C., Mante, V., Simoncelli, E. P. & Movshon, J. A. (2006). How MT cells analyze the
531 motion of visual patterns. *Nature Neuroscience*, 9(11), 1421-1431.

532 Smith, M. A., Majaj, N. J. & Movshon, J. A. (2005). Dynamics of motion signaling by neurons
533 in macaque area MT. *Nature Neuroscience*, 8(2), 220-228.

534 Simoncelli, E. P. & Heeger, D. J. (1998). A model of neuronal responses in visual area MT.
535 *Vision Research*, 38(5), 743-761.

536 Sincich, L. C., Park, K. F., Wohlgenuth, M. J., & Horton, J. C. (2004). Bypassing V1: a direct
537 geniculate input to area MT. *Nature Neuroscience*, 7(10), 1123.

538 Taouali, W., Benvenuti, G., Wallisch, P., Chavane, F., & Perrinet, L. U. (2015). Testing the odds
539 of inherent vs. observed overdispersion in neural spike counts. *Journal of Neurophysiology*,
540 115(1), 434-444.

541 Wallach, H. (1935). Über visuell wahrgenommene Bewegungsrichtung. *Psychological Research*,
542 20(1), 325-380.

543 Wilson, H. R., Ferrera, V. P. & Yo, C. (1992). A psychophysically motivated model for two-
544 dimensional motion perception. *Visual Neuroscience*, 9(1), 79-97.

545 Yo, C. & Wilson, H. R. (1992). Perceived direction of moving two-dimensional patterns depends
546 on duration, contrast and eccentricity. *Vision Research*, 32(1), 135-147.

547 Zaharia, A. D., Goris, R. L., Movshon, J. A. & Simoncelli, E. P. (2019). Compound stimuli
548 reveal the structure of visual motion selectivity in macaque MT neurons. *bioRxiv* doi:
549 10.1101/692533.

550

551

552 **Figure legends**

553 Figure 1: The intersection of constraints in velocity space, illustrated for bikineti-
554 c and unikinetic plaid stimuli. The perceived motion of visual patterns can be understood within an “intersection
555 of constraints” (IOC) framework. An individual grating is perceived as moving orthogonal to its
556 orientation, depicted by the black arrows, but this stimulus is also consistent with any number of
557 faster-moving gratings that share the same orthogonal component, indicated by grey arrows. The
558 endpoints of these arrows, taken together, form a constraint line in velocity space (dashed lines).
559 Connecting the origin of this velocity space with the point where the constraint lines intersect
560 yields the vector (red arrow) that corresponds to the true motion of the stimulus, and to the
561 percept of an unbiased observer who sees the two gratings superimposed. In the case of bikineti-
562 c plaids (A), two moving gratings of equal speed are superimposed, so the constraint lines intersect
563 on the horizontal axis, giving the percept of a stimulus moving to the right. In the unikinetic case
564 (B), one moving and one static grating are superimposed. The constraint line imposed by the
565 static grating goes through the origin, shifting the intersection point of the constraint lines 30° off
566 the horizontal, towards the veridical motion vector of the moving grating. The lengths of the red
567 arrows indicate that the unikinetic plaid moves more slowly than the bikineti-
568 c one.

569 Figure 2: Example responses of pattern and component cells to gratings and plaids. A: The
570 curves in the center of each stimulus family show the predicted responses of idealized pattern
571 (red) and component (blue) selective neurons tuned for rightward motion when tested with the
572 stimuli depicted in the ring. These correspond to the conditions used in our experiment. All
573 conditions were tested in 12 directions, though for economy the full set is only shown here for
574 the static case. The five parts of each panel show responses to different sets of targets. *Stationary*
575 *gratings*: MT neurons are generally not strongly responsive or selective for static patterns, so we
576 expect only weak responses, not differing between pattern and component cells and indicated in
577 black. *Moving gratings*: We expect both pattern and component cells to exhibit a robust
578 unimodal response, represented by the black von Mises function in the center. The motion of
579 each grating is indicated by black arrows. *Bikineti- c plaids*: As in Fig 1A, these consist of two
580 moving component gratings (the motion of which is indicated by blue arrows) yielding one
581 pattern motion (red arrows). We expect pattern and component cells to exhibit bimodal
582 (component cell) and unimodal (pattern cell) tuning, represented by blue and red von Mises

583 functions. *Left- and right-handed unikinetic plaids*: As in Fig 1B, these consist of a moving
584 grating and a stationary one, the left- and right-handed cases differ in which grating is moving.
585 The color scheme is the same as in the case of the bikinetic plaid. We expect both pattern and
586 component cells to exhibit unimodal tuning. The component cells should respond to the moving
587 grating essentially as if the static grating were absent. We therefore expect a difference in
588 preferred direction of 60° between the two kinds of unikinetic plaid. Pattern cells' tuning should
589 be aligned with the pattern motion, and the difference in preferred directions should be roughly
590 0° . B-E: Responses of four representative example cells. Color scheme as in A, but the pattern
591 and component predictions are depicted in dashed lines whereas the measured responses are
592 drawn in solid lines. All cells responded weakly to static gratings and showed classical response
593 characteristics to moving gratings and bikinetic plaids. The component cell (B) responded in a
594 fashion consistent with the component prediction (the direction tuning rotation was 52°). The
595 pattern cells (D, E) obeyed the pattern prediction, although not perfectly (direction tuning
596 rotation values of 7 and 16° , respectively). The mixed cell (C) showed classical behavior to
597 moving gratings and bikinetic plaids, and would be classified as a pattern cell when stimulated
598 with bikinetic plaids, but when probed with unikinetic plaids, it showed component cell-like
599 behavior (direction tuning rotation of 38°).

600

601 Figure 3: Pattern/component classification for bi- and unikinetic plaids. A: Bikinetic plaids. The
602 ordinate represents the partial correlation of the neural response with the pattern prediction (Z_p),
603 the abscissa represents the partial correlation of neural response with the component prediction
604 (Z_c). Black lines indicate the borders of significance that allow a statistical classification of cell
605 behavior. Pattern cells (falling in the upper region) are drawn in red and component cells (falling
606 in the lower region) are drawn in blue, unclassified cells (falling between these regions) are drawn
607 in black. Open circles indicate that the cell was recorded in the acute preparation, filled circles
608 indicate that the cell was recorded under awake conditions. Black circles indicate the example
609 cells from Fig 2. B: Unikinetic plaids (averaged over both left- and right-handed unikinetic
610 conditions). The cells are colored based on their classification determined with bikinetic plaids.

611

612 Figure 4: Pattern index predicts the rotation of direction preference induced by static stimuli. The
613 abscissa gives the pattern index ($Z_p - Z_c$) for bikinetic plaids, the ordinate gives the direction

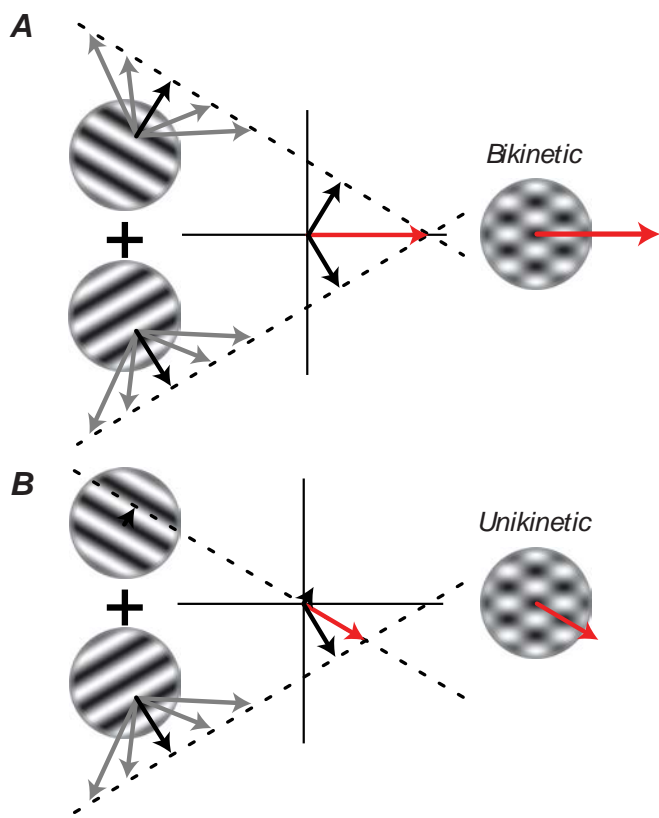
614 preference difference between responses to left- and right-handed unikinetic plaids. Orange
615 represents data from the alert animal and green represents data from the anesthetized animals; the
616 error bars represent the bootstrapped standard deviations of the estimates for pattern index and
617 rotation. The solid lines represent the lines of best fit (Press et al., 1992) for the two groups of
618 cells. Arrows show the direction tuning rotation expected from idealized pattern and component
619 cells (Fig 2A). Black circles indicate the example cells from Fig. 2. The shaded background
620 colors indicate the ranges of pattern and component cells as displayed in Fig. 3.

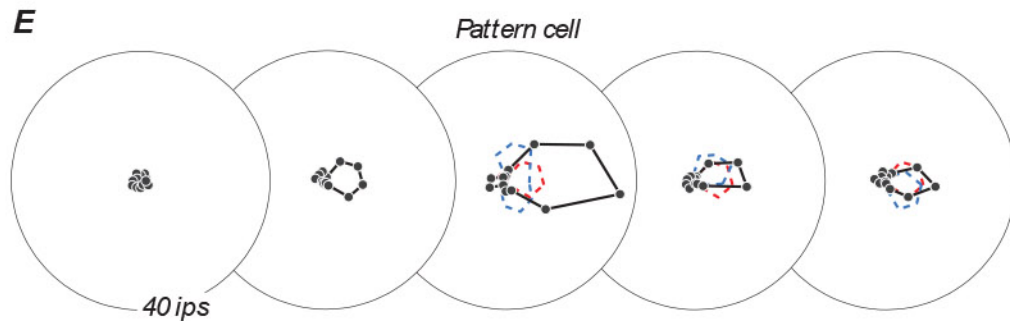
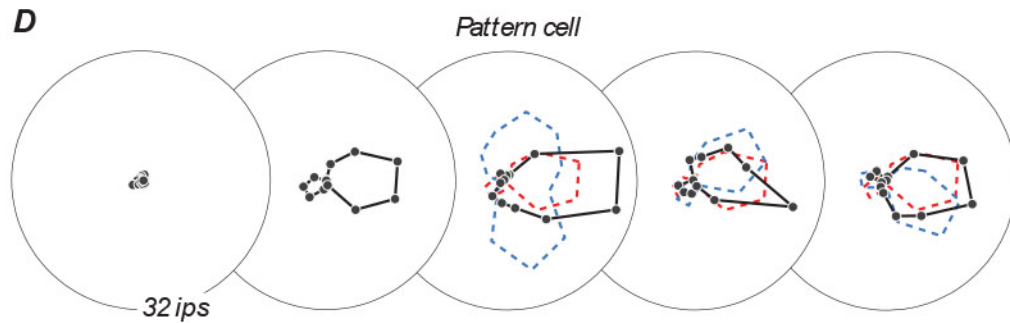
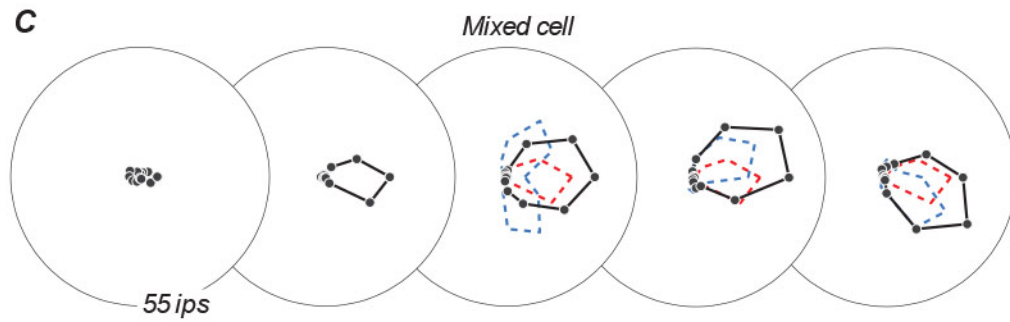
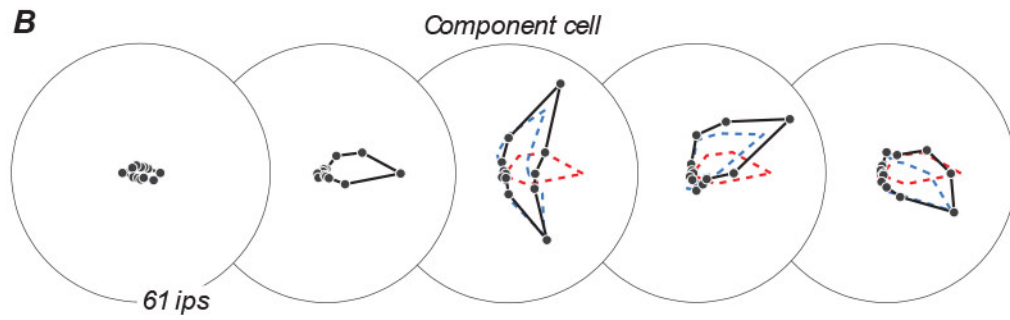
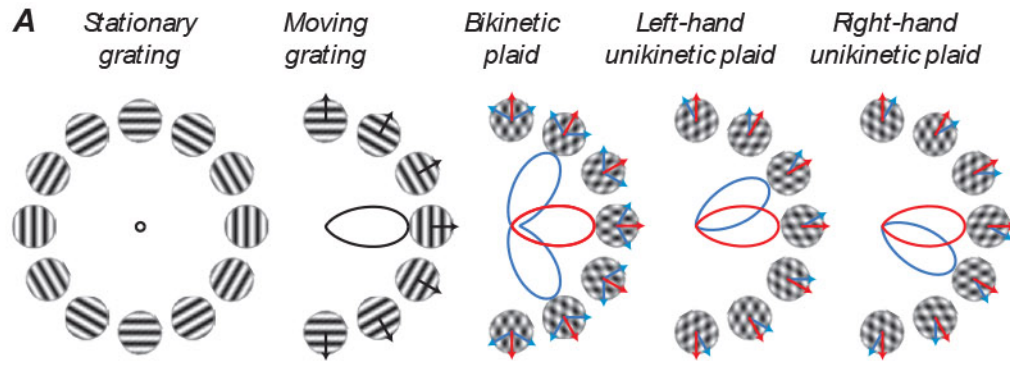
621

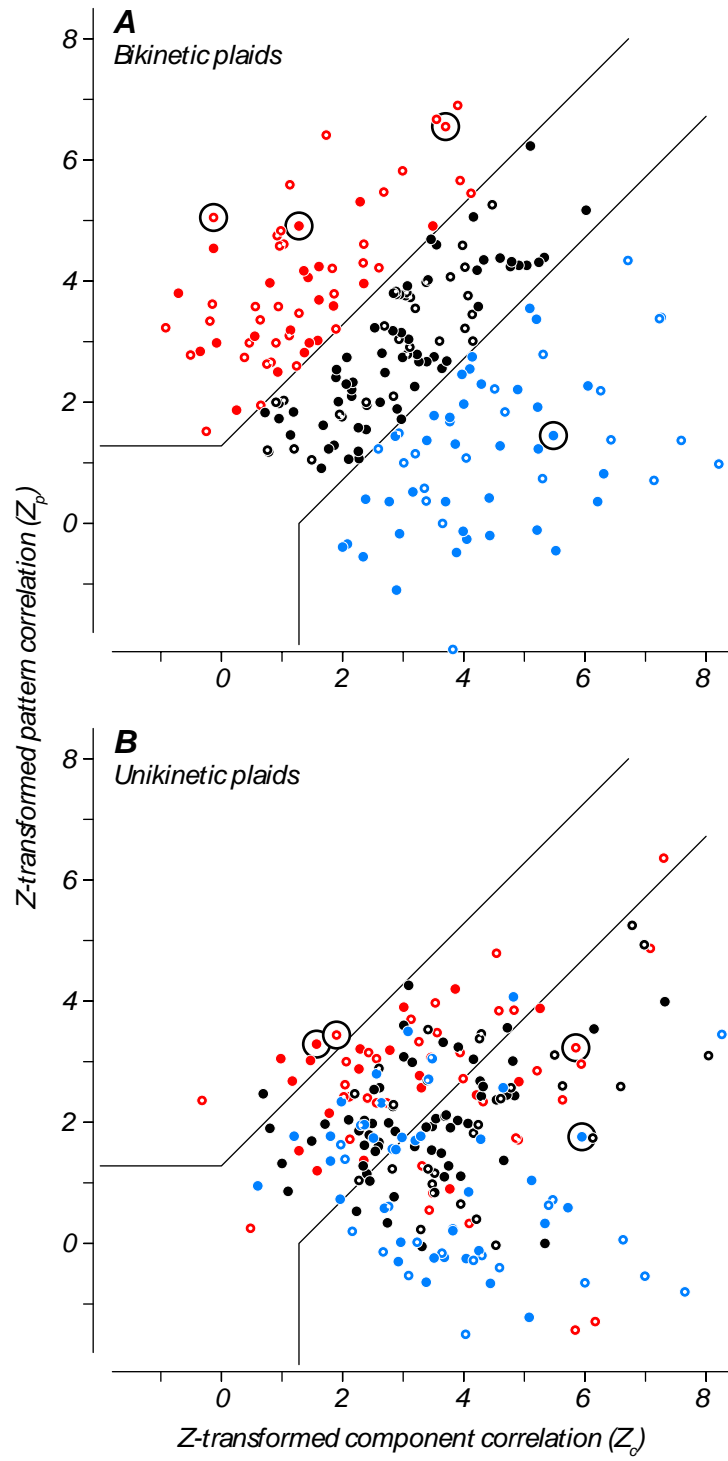
622 Figure 5: Time course of responses and tuning preferences for asynchronously presented
623 compound stimuli. A: Experimental design. At the start of all trials, we introduced a static
624 grating (gray arrow). For trials with compound stimuli, we added a moving grating with an
625 orientation 60° different from the static grating either synchronously (red), or with a delay of 50
626 or 100 ms (blue, cyan). B, C: Mean firing rates evoked by optimal single gratings and plaids
627 containing those gratings for 121 cells from alert animal (B) and for 84 cells from the
628 anesthetized animal (C) for the four stimulus conditions schematized in A, computed at 1 ms
629 intervals within a 5 ms sliding window. D, E: Mean direction tuning to moving stimuli for the
630 neuronal populations (anesthetized: D, alert: E). We rotated the tuning data for all neurons so
631 that the preferred direction for single gratings was aligned at horizontal (here indicated as 30°),
632 and estimated the population preferred direction within the same 5 ms sliding window. The
633 preferred direction is plotted only for times past the time at which the estimate for each stimulus
634 had stabilized.

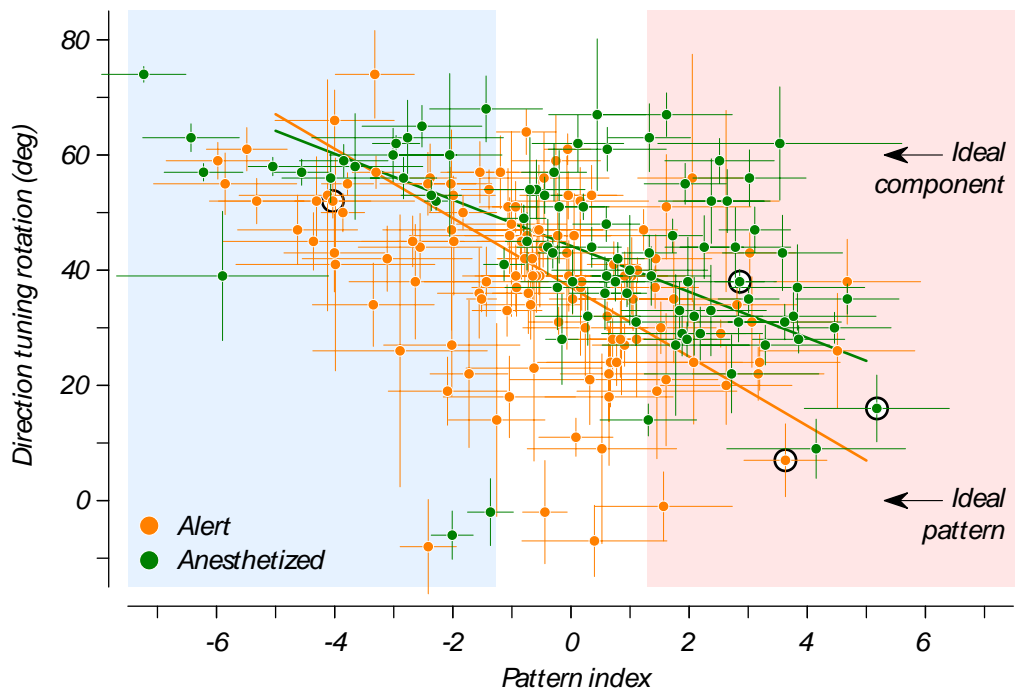
635

636









A